Inertial particle under active fluctuations: Diffusion and work distributions

Koushik Goswami
Department of Chemistry, Indian Institute of Technology Bombay, Mumbai, Powai 400076, India
and Institute of Physics & Astronomy, University of Potsdam, Karl-Liebknecht-Straße 24/25, 14476 Potsdam-Golm, Germany

(Received 2 December 2021; accepted 30 March 2022; published 15 April 2022)

We study the underdamped motion of a passive particle in an active environment. Using the phase space path integral method we find the probability distribution function of position and velocity for a free and a harmonically bound particle. The environment is characterized by an active noise which is described as the Ornstein-Uhlenbeck process (OUP). Taking two similar, yet slightly different OUP models, it is shown how inertia along with other relevant parameters affect the dynamics of the particle. Further we investigate the work fluctuations of a harmonically trapped particle by considering the trap center being pulled at a constant speed. Finally, the fluctuation theorem of work is validated with an effective temperature in the steady-state limit.

DOI: 10.1103/PhysRevE.105.044123

I. INTRODUCTION

Over the past few decades, there has been a growing interest in understanding active particles from their dynamical and energetic perspective. An active particle is basically a system that moves on its own harnessing the energy from its environment. Recently, it has been widely studied due to its applicability and ubiquitous presence in nature, e.g., from swarming bacteria to flocking of birds—all these phenomena can be perceived within the purview of active matters [1–5]. The models that have been extensively used to describe the processes are active Brownian particles (ABP) [6–8], active Ornstein-Uhlenbeck particles (AOUPs) [9–12], and run-and-tumble particles (RTPs) [13–15]. Most of the studies with these models deal with the overdamped dynamics of such particles which neglects inertial contributions due to their movement in a fluid at a low Reynolds number. However, for a self-driven particle moving in a low-density environment such as in a gaseous medium, or for a particle with a large Stokes number, its motion is inertia-dominated and thus its self-propulsion gets coupled with inertial effects displaying distinctive, nonlinear behavior [16]. For instance, inertia of squirmers such as marine plankton changes their swimming speed depending on the location of thrust generation, and it also induces hydrodynamic interaction between two squirmers [17,18]. Some other natural realizations where inertia is important include insect aerial flight, swimming of living organisms in water, autorotating motion of helicopter fruits in air, etc. [19–22]. With recent advances in constructing artificial self-propelled objects, the field of active matters in the underdamped regime (at intermediate and high Reynolds numbers) has been further invigorated from the experimental point of view. Examples of such objects are rotating robots, vibrobots, artificial bugs, to name a few [23–25].

More recently, several groups have theoretically investigated the underdamped motion of self-propelled particles [26–29]. In Ref. [26], it has been elucidated theoretically that inertia of a self-propelled particle induces a delay between orientation and its velocity, which has been experimentally observed earlier [24]. Recently, Löwen *et al.* have studied the self-organization of repulsively interacting active particles with inertia, famously known as "motility-induced phase separation" (MIPS) where it has been found that there coexists two phases, but with two different kinetic temperatures, termed as "hot-cold coexistence," which is missing in the overdamped description [30]. In other studies, the effect of inertia on several properties such as mean-square displacement (MSD), mean-square speed, and swim pressure has been investigated [27,28,31,32].

In recent years, studies on passive particles immersed in an active environment have received a considerable attention [33–35]. However, its motion in the underdamped limit remains almost unexplored. Like a single active particle, it can also be modeled in a simplistic way by the Ornstein-Uhlenbeck process (OUP) where the particle is subjected to Gaussian driving with a finite correlation time [36,37]. Note that the OUP model has been widely used as it turns out to be successful in explaining some interesting collective behavior of self-propelled particles such as accumulation near boundaries and MIPS [38,39]. In this paper, we study the dynamics of a passive particle in the underdamped limit in a fluid as it experiences active noise which are characterized here by the OU process. We consider two OUP models with slight variations in the strength of the noise. Though the treatments for both models are the same, the results as well as interpretations may differ. The dynamics along with OUP models are discussed in Sec. II. With these models, the motion of a free particle and a harmonically confined particle is investigated theoretically. Employing the phase-space path integral (PSPI) method, we find exact results for the probability distribution function in position and velocity, and then we analyze the effects of relevant dynamical variables, as discussed in Sec. III. It is worth mentioning here that though our discussions will mostly be focused on dynamics of a passive particle in an active bath, the formalism presented here can be applicable to an active inertial particle as well. For such cases, the active noise corresponds to the swim (or self-propulsion) velocity which has a fixed average value, e.g., see Ref. [27].

It is well established that the particle subjected to active fluctuations is driven out of equilibrium. In other words, detailed balance as well as fluctuation-dissipation relation break down. Recently, it has been found experimentally as well as theoretically that the fluctuation theorems (FT), in general, do not hold for such systems, but a specific kind of relation do exist in the steady-state limit [33,40,41]. Work fluctuations and related FTs in equilibrium baths have been studied previously by few groups in the underdamped limit [42–44]. However, in active baths and at intermediate and high Reynolds numbers, similar studies are lacking. Along these lines, there have been some recent studies which looked into the stochastic energetics of inertial active systems [45,46]. As previous studies suggest, the steady state of active systems can be mapped to an effective equilibrium, and therefore, thermodynamic variables may follow equivalent equilibrium properties with renormalized parameters. In Sec. IV, we study work fluctuations for a specific protocol, and compute the work distribution using the PSPI technique. Then we verify the fluctuation theorem of work in the underdamped limit. All results are summarized in Sec. V. Other useful information in support of the main results is presented in Appendices. The characteristic functional for the OU process is derived in Appendix A. For the sake of completeness, some preliminary idea on the path integration method is discussed in Appendix B. The complete expressions of distributions in position and velocity are shown in Appendix C, and the detailed calculation of work distribution is given in Appendix D.

II. DYNAMICS

Here we consider that a passive particle is diffusing under a potential $U(x)$ in a bath containing active particles at temperature T. So in addition to the thermal fluctuations, an active force is present in the environment, thereby referring to it as an active bath. Without neglecting the inertial contribution to the dynamics of the particle, the stochastic equation for its motion in the underdamped limit can be expressed as

$$\frac{1}{\gamma}\ddot{x}(t) + \dot{x}(t) + \frac{U'[x(t),t]}{m\gamma} = \eta_T(t) + \eta_A(t). \tag{1}$$

Here the first term accounts for the inertial force, and m is the mass of the particle. The drag force is given by $m\gamma\dot{x}$, where γ is the viscosity coefficient which is related to the diffusion coefficient D_T due to the presence of thermal noise $\eta_T(t)$ only, through the Einstein relation $D_T = \frac{k_B T}{m\gamma}$, with k_B being the Boltzmann constant. Naturally, the (second) fluctuation-dissipation theorem (FDT) follows: $\langle\eta_T(t)\eta_T(t')\rangle = 2D_T\delta(t-t')$. Henceforth, the mass m is taken to be unity. The active force is denoted here as $\eta_A(t)$, which introduces nonequilibrium elements to the system. In the following two models of $\eta_A(t)$ are discussed.

Here $\eta_A(t)$ is taken as a Gaussian colored noise whose evolution can be described by the Ornstein-Uhlenbeck process (OUP) [47,48], viz.,

$$\dot{\eta}_A(t) = -\frac{1}{\tau_A}\eta_A(t) + \frac{1}{\tau_A}\xi(t), \tag{2}$$

where $\xi(t)$ is the white Gaussian noise obeying $\langle\xi(t)\rangle = 0$ and $\langle\xi(t)\xi(t')\rangle = 2D_A(t-t')$, with D_A being the active diffusivity, that is, the diffusion coefficient when the particle diffuses only in the presence of active noise $\eta_A(t)$. From Eq. (2) one can see that $\langle\eta_A(t)\rangle = 0$ and $\langle\eta_A(t_1)\eta_A(t_2)\rangle = \frac{D_A}{\tau_A}e^{-\frac{|t_1-t_2|}{\tau_A}}$, τ_A being the persistence time of the active noise. Notice that, for a very small persistence time, i.e., for $\tau_A \to 0$, the noise $\eta_A(t)$ becomes δ-correlated, and so it behaves like a Gaussian white noise.

The other way to realize $\eta_A(t)$ is by writing a dynamical equation similar to OUP for the active force $f_A(t)$, where $f_A(t) = \gamma\eta_A(t)$, as follows [11,27]:

$$\dot{f}_A(t) = -\frac{1}{\tau_A}f_A(t) + \sqrt{\frac{1}{\tau_A}}\xi_A(t), \tag{3}$$

where $\langle\xi_A(t)\rangle = 0$ and $\langle\xi_A(t)\xi_A(t')\rangle = 2f_0^2\delta(t-t')$, which implies that $\langle f_A(t_1)f_A(t_2)\rangle = f_0^2 e^{-\frac{|t_1-t_2|}{\tau_A}}$. The average of active force $f_A(t)$ is denoted here as f_0, and its value is considered to be fixed in this model. It is relevant when a system in motion (e.g., a self-propelled particle) maintains a constant average speed throughout its journey. Now it is easy to see that the autocorrelation of $\eta_A(t)$ is also an exponential function of the form $\langle\eta_A(t_1)\eta_A(t_2)\rangle = \frac{f_0^2}{\gamma^2}e^{-\frac{|t_1-t_2|}{\tau_A}}$. In the limit $\tau_A \to 0$, the noise disappears, which clearly differs from the OUP model [Eq. (2)] discussed earlier. To distinguish it from the previous OUP model, one may term it [Eq. (3)] as the modified Ornstein-Uhlenbeck process, or in short, MOUP model. Notice that one can map these two models by defining the strengths of the autocorrelation functions in such as way that $D_A = \frac{f_0^2}{\gamma^2}\tau_A$. It is useful to note that the characteristic functional of the noise $\eta_A(t)$ corresponding to any of these models can be calculated using the relation [49]

$$\langle e^{i\int_0^t dt_1\, p(t_1)\eta_A(t_1)}\rangle_{\eta_A} = e^{-\frac{1}{2}\int_0^t dt_1\int_0^t dt_2\, p(t_1)\langle\eta_A(t_1)\eta_A(t_2)\rangle p(t_2)}, \tag{4}$$

where $p(t)$ is the conjugate variable to η_A, and the angular bracket $\langle\cdots\rangle$ denotes the average over all histories of $\eta_A(t)$. For the sake of clarity, an alternative derivation of Eq. (4) considering an exponential correlation of $\eta_A(t)$ is provided in Appendix A.

III. PROBABILITY DISTRIBUTION FUNCTION OF DISPLACEMENT x AND VELOCITY v

Here we compute the probability distribution function (PDF) of finding the particle at some position x at time t. To do so, we employ the PSPI method [50,51] (see also Appendix B), and write the probability density functional for the white noise $\eta_T(t)$ as

$$\mathbb{P}[\eta_T] = \int \mathcal{D}p e^{-D_T \int_0^t dt_1 p^2(t_1) - i\int_0^t dt_1\, p(t_1)\eta_T(t_1)}, \tag{5a}$$

$$\mathbb{P}[x] \sim \int \mathcal{D}p e^{-D_T \int_0^t dt_1 p^2(t_1) - i\int_0^t dt_1\, p(t_1)}\left\{\frac{1}{\gamma}\ddot{x}(t_1)+\dot{x}(t_1)+\frac{U'[x(t_1),t_1]}{\gamma}-\eta_A(t_1)\right\}, \tag{5b}$$

$$\mathbb{P}[x] = \int \mathcal{D}p e^{-D_T \int_0^t dt_1 p^2(t_1)}\, \langle e^{i\int_0^t dt_1\, p(t_1)\eta_A(t_1)}\rangle_{\eta_A}\, e^{-i\int_0^t dt_1\, x(t_1)[\frac{1}{\gamma}\ddot{p}(t_1)-\dot{p}(t_1)]} e^{-\frac{i}{\gamma}\int_0^t dt_1\, p(t_1)U'[x(t_1),t_1]}$$
$$\times\, e^{-\frac{i}{\gamma}[\dot{x}(t)p(t)-\dot{x}(0)p(0)]-ix(t)[p(t)-\frac{1}{\gamma}\dot{p}(t)]+ix(0)[p(0)-\frac{1}{\gamma}\dot{p}(0)]}. \tag{5c}$$

In Eq. (5b), we have replaced $\eta_T(t)$ by using Eq. (1) and consequently, the functional has been expressed in terms of trajectories of $x(t)$. In Eq. (5c), integration by parts has been performed. As $\eta_A(t)$ evolves independently of $x(t)$, one needs to do the averaging over all trajectories of $\eta_A(t)$, and the average is denoted by the angular bracket in Eq. (5c). Therefore, the PDF (or the propagator) can be obtained on doing the path integration over $x(t)$, and it reads

$$P(x_t, v_t, t; x_0, v_0, 0) = \int_{x(0)=x_0}^{x(t)=x_t} \mathcal{D}x \int \mathcal{D}p e^{-D_T \int_0^t dt_1 p^2(t_1)} \langle e^{i\int_0^t dt_1\, p(t_1)\eta_A(t_1)}\rangle_{\eta_A}\, e^{-i\int_0^t dt_1\, x(t)[\frac{1}{\gamma}\ddot{p}(t_1)-\dot{p}(t_1)]}$$
$$\times\, e^{-\frac{i}{\gamma}\int_0^t dt_1\, p(t_1)U'[x(t_1),t_1]} e^{-\frac{i}{\gamma}[v_t p(t)-v_0 p(0)]-ix_t[p(t)-\frac{1}{\gamma}\dot{p}(t)]+ix_0[p(0)-\frac{1}{\gamma}\dot{p}(0)]}, \tag{6}$$

where $v_t = \dot{x}(t)$, $v_0 = \dot{x}(0)$. With this formalism, we study the dynamics of the particle in two different potentials.

A. Free particle, $U(x) = 0$

Taking $U(x) = 0$ and $x_0 = 0$ in Eq. (6), the PDF can be written as

$$P(x_t, v_t, t; v_0) = \int_{x(0)=0}^{x(t)=x_t} \mathcal{D}x \int \mathcal{D}p e^{-D_T \int_0^t dt_1 p^2(t_1)}$$
$$\times\, \langle e^{i\int_0^t dt_1\, p(t_1)\eta_A(t_1)}\rangle_{\eta_A} e^{-i\int_0^t dt_1\, x(t_1)[\frac{1}{\gamma}\ddot{p}(t_1)-\dot{p}(t_1)]}$$
$$\times\, e^{-\frac{i}{\gamma}[v_t p(t)-v_0 p(0)]-ix_t[p(t)-\frac{1}{\gamma}\dot{p}(t)]}. \tag{7}$$

The path integration over x produces a δ functional, $\delta[\ddot{p}(t_1) - \gamma\dot{p}(t_1)]$, which implies $p(t_1) = (\frac{p_t-p_0e^{\gamma t}}{1-e^{\gamma t}}) + (\frac{p_0-p_t}{1-e^{\gamma t}})e^{\gamma t_1}$, $p(0) = p_0$, $p(t) = p_t$. Therefore, the path integration over p becomes a double integration with respect to p_0 and p_t, and so Eq. (7) can be rewritten as

$$P(x_t, v_t, t; x_0, v_0, 0)$$
$$= \int dp_t \int dp_0\, e^{-D_T \int_0^t dt_1 p^2(t_1)} \langle e^{i\int_0^t dt_1\, p(t_1)\eta_A(t_1)}\rangle_{\eta_A}$$
$$\times\, e^{-\frac{i}{\gamma}(v_t p_t - v_0 p_0)-ix_t(p_t-\frac{1}{\gamma}\dot{p}_t)} \tag{8}$$

Using Eq. (4) the ensemble average over η_A can be calculated. With this, the probability distribution function of finding the particle at position x_t with velocity v_t at time t provided that the initial velocity v_0 follows the Boltzmann distribution, $\mathcal{P}(v_0) = \sqrt{\frac{1}{2\gamma\pi D_T}}\, e^{-\frac{1}{2\gamma D_T}v_0^2}$ and $P(x_0) = \delta(x_0)$, can be computed as

$$P(x_t, v_t, t) = \int dx_0 \int dv_0 P(x_t, v_t, t; x_0, v_0, 0)P(v_0)P(x_0)$$
$$= \sqrt{\frac{1}{(2\pi)^2|\mathbb{C}_f|}}\, e^{-\frac{1}{2}\mathbb{X}^T\mathbb{C}_f^{-1}\mathbb{X}}, \tag{9}$$

with $|\mathbb{C}_f|$ being the determinant of the matrix $\mathbb{C}_f$ as given in Appendix C 1. The PDF for velocity v_t considering the final position x_t to be anywhere in the space can be obtained as

$$P(v_t, t) = \int dx_t P(x_t, v_t, t) = \sqrt{\frac{1}{2\pi\sigma_v^2(t)}}\, e^{-\frac{v_t^2}{2\sigma_v^2(t)}}, \tag{10}$$

where $\sigma_v^2(t)$ is the variance of velocity v_t, expressed as

$$\sigma_v^2(t) = \gamma \frac{e^{-t(2\gamma+\frac{1}{\tau_A})}}{(\gamma^2\tau_A^2-1)}[(\gamma\tau_A - 1)e^{t(2\gamma+\frac{1}{\tau_A})}$$
$$\times\, (\gamma D_T\tau_A + D_T + D_A) - 2D_A\gamma\tau_A e^{\gamma t}$$
$$+ D_A(\gamma\tau_A + 1)e^{t/\tau_A}].$$

In the long time limit, i.e., for $t \gg \frac{1}{\gamma}$ and $t \gg \tau_A$, the variance is given by

$$\sigma_v^2 = \lim_{\gamma t\gg 1; t/\tau_A\gg 1} \sigma_v^2(t) = D_T\gamma + \frac{D_A}{\tau_A}\frac{\gamma\tau_A}{\gamma\tau_A + 1}. \tag{11}$$

So in the OUP bath, it has the stationary probability distribution function of velocity associated with an effective temperature $D_T + \frac{D_A}{\gamma\tau_A+1}$. Notice that in the absence of active noise η_A, $\sigma_v^2(t) \approx D_T\gamma = k_BT$, which means that the system remains in equilibrium, thereby having the Boltzmann distribution. For the case where the persistence time (τ_A) is very small compared to the inertial time $1/\gamma$, i.e., for $\gamma\tau_A \ll 1$, the system can still be understood through the equilibrium theory incorporating an effective temperature $T_{\text{eff}} = T + T_A$, where $T_A = D_A\gamma$. Now one can compute the distribution of displacement as

$$P(x_t, t) = \int dv_t P(x_t, v_t, t) = \sqrt{\frac{1}{2\pi\sigma_x^2(t)}}\, e^{-\frac{x_t^2}{2\sigma_x^2(t)}}, \tag{12}$$

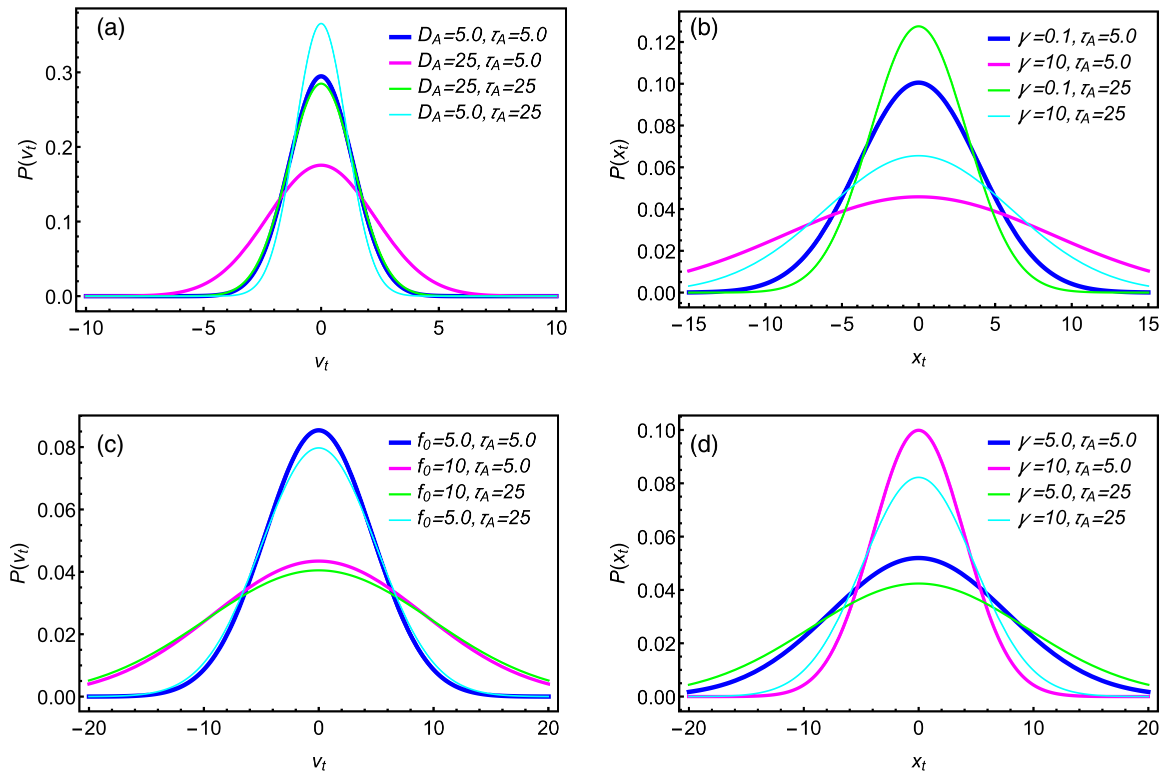

FIG. 1. Plots of the probability distribution function (PDF) for the free particle in panels (a, b) the OUP bath, and in panels (c, d) the MOUP bath. The PDFs of velocity v_t [given in Eq. (10)] are plotted as a function of v_t at time $t = 10$ for different values of τ_A in panels (a, c) for the OUP and MOUP models, respectively. In panel (a) the values of fixed parameters are $\gamma = 1.0,\ D_T = 1.0$ while varying the values of D_A, whereas in the panel (c) f_0 is varied, keeping the other parameters constant at $T = 1.0,\ \gamma = 1.0$. Panels (b, d) show the PDFs of displacement x_t [given in Eq. (12)] at time $t = 10$ in the OUP and MOUP baths, respectively. In panel (b) the fixed parameters are $D_T = 1.0,\ D_A = 5.0$, and in panel (d) we have taken $T = 1.0,\ f_0 = 5$.

where

$$\sigma_x^2(t) = \frac{\gamma\, e^{-t\left(2\gamma+\frac{1}{\tau_A}\right)}}{\left(\gamma^2\tau_A^2-1\right)}\Big[-2\gamma^2 D_A\tau_A^2 e^{\gamma t} + 2\gamma^2 D_A\tau_A^2 e^{2\gamma t}(\gamma\tau_A+1) + D_A(\gamma\tau_A+1)e^{\frac{t}{\tau_A}} + 2(\gamma\tau_A+1)$$
$$\times\ e^{t\left(\frac{1}{\tau_A}+\gamma\right)}[\gamma\tau_A(D_A+D_T) - 2D_A - D_T] + (\gamma\tau_A-1)e^{t\left(\frac{1}{\tau_A}+2\gamma\right)}(D_A\{2\gamma[-\tau_A(\gamma\tau_A+2)+\gamma t\tau_A+t]$$
$$-\,3\} + 2D_T(\gamma t-1)(\gamma\tau_A+1))\Big].$$

In the long-time limit, the MSD can be expressed as

$$\lim_{\gamma t\gg 1;\, t/\tau_A\gg 1} \sigma_x^2(t) \approx 2(D_T + D_A)t. \tag{13}$$

This suggests a diffusive behavior with enhanced diffusivity. For short times, i.e., for $\gamma t \ll 1,\ t/\tau_A \gg 1,\ \sigma_x^2(t) \approx D_T\gamma t^2$, indicating a ballistic regime due to thermal fluctuations. However, if one considers that initial velocity had a nonequilibrium stationary distribution with the effective temperature given in Eq. (11), then active fluctuations contribute to the ballistic behavior, viz., $\sigma_x^2(t) \approx (D_T\gamma + \frac{D_A}{\tau_A}\frac{\gamma\tau_A}{\gamma\tau_A+1})t^2$. This is consistent with the recent result reported in Ref. [27] for a self-propelled particle with inertia. The results for the MOUP bath can also be obtained in a similar way as discussed above. The only change one needs to do is to replace D_A by the term $\frac{f_0^2}{\gamma^2}\tau_A$. However, the role of dynamical parameters differs in these two models. For example, in the limit $\gamma\tau_A \gg 1,\ \sigma_v^2 \propto \frac{1}{\tau_A}$ for the OUP model, whereas σ_v^2 has no dependence on τ_A for the MOUP model and is given by $\sigma_v^2 \approx T + \frac{f_0^2}{\gamma^2}$.

The marginal distributions of x_t and v_t for the free particle are plotted in Fig. 1. In the OUP bath, the width of the distribution of v_t grows with D_A for fixed persistence time τ_A, as the presence of active noise results in an enhanced diffusivity. However, the width becomes narrower as τ_A increases, as shown in Figs. 1(a) and 1(b) for the distribution of x_t. One can also observe from Fig. 1(b) that the spatial distribution has a wider spread for a large value of γ and fixed values of diffusivities as the effective temperature is also increased. Figure 1(c) shows the distribution of velocity in the MOUP bath for different values of active force f_0 and τ_A, keeping D_T and γ fixed. Evidently the particle travels a longer distance on average as f_0 takes a higher value. In contrast to the OUP model, the widths—$\sigma_x^2(t)$ and $\sigma_v^2(t)$ decrease as the motion transits from the underdamped to an overdamped regime (with the increment of γ) as well as with the decrease of τ_A, as can be viewed in Fig. 1(d). It suggests that τ_A and $1/\gamma$ play a similar role in both models.

B. In a harmonic potential, $U(x) = \frac{\lambda}{2}x^2$

Here we consider the dynamics of a particle in a harmonic potential of the form: $U(x) = \frac{\Lambda}{2}x^2$, with stiffness Λ. From Eq. (6), the propagator can be expressed as

$$P(x_t, v_t, t; x_0, v_0, 0) = \int_{x(0)=x_0}^{x(t)=x_t} \mathcal{D}x \int \mathcal{D}p e^{-D_T \int_0^t dt_1 p^2(t_1)} \langle e^{i\int_0^t dt_1\, p(t_1)\eta_A(t_1)}\rangle_{\eta_A} e^{-i\int_0^t dt_1\, x(t_1)[\frac{1}{\gamma}\ddot{p}(t_1)-\dot{p}(t_1)+\lambda p(t_1)]} \times e^{-\frac{i}{\gamma}[v_t p(t)-v_0 p(0)]-ix_t[p(t)-\frac{1}{\gamma}\dot{p}(t)]+ix_0[p(0)-\frac{1}{\gamma}\dot{p}(0)]}, \quad (14)$$

where $\lambda = \Lambda/\gamma$. Doing the path integration over x, one gets $p(t_1) = p_t e^{-\frac{\gamma}{2}(t-t_1)}\sinh(\frac{\Gamma t_1}{2})\text{csch}(\frac{\Gamma t}{2}) + p_0\, e^{\frac{\gamma}{2}t_1}[\cosh(\frac{\Gamma t_1}{2}) - \sinh(\frac{\Gamma t_1}{2})\cosh(\frac{\Gamma t}{2})\text{csch}(\frac{\Gamma t}{2})]$, where $\Gamma = \sqrt{\gamma(\gamma-4\lambda)}$. Therefore, the functional integration over p reduces to a double integration with respect to p_0 and p_t, viz.,

$$P(x_t, v_t, t; x_0, v_0, 0) = \int dp_t \int dp_0\, e^{-D_T\int_0^t dt_1 p^2(t_1)}\langle e^{i\int_0^t dt_1\, p(t_1)\eta_A(t_1)}\rangle_{\eta_A} \times e^{-\frac{i}{\gamma}[v_t p(t)-v_0 p(0)]-ix_t[p(t)-\frac{1}{\gamma}\dot{p}(t)]+ix_0[p(0)-\frac{1}{\gamma}\dot{p}(0)]}. \quad (15)$$

Here we only consider the case where $\gamma > 4\lambda$. One may also take the opposite case, viz. $\gamma < 4\lambda$, for which Γ is a complex quantity and so some distinct properties such as oscillations in the time correlations of $x(t)$ may be observed, but for our present work, the analysis with the first case serves the purpose. Now, Eq. (15) can be computed exactly, and using the result, the PDFs in x_t and v_t can be found easily as shown in Appendix C 2.

Now we analyze the stationary limit by taking $t \to \infty$. From Eq. (C3) the PDF of velocity at the steady state can be written as

$$P_{\text{st}}(v_t) = \sqrt{\frac{1}{2\pi\gamma\big(D_T + \frac{D_A}{1+\gamma\tau_A+\gamma\lambda\tau_A^2}\big)}} \times \exp\left[-\frac{v_t^2}{2\gamma\big(D_T+\frac{D_A}{1+\gamma\tau_A+\gamma\lambda\tau_A^2}\big)}\right]. \quad (16)$$

Note that the system follows the above distribution whether it is initially at equilibrium or it evolves from a nonequilibrium stationary state. Notice that, in the absence of active noise η_A, it again follows the Boltzmann distribution with the ambient temperature, which is a quick test of the correctness of our result. Let us now check a few other cases. For an unconfined particle, $\lambda \to 0$, and the distribution becomes $\lambda-$ independent, viz., $P(v_t) \approx \sqrt{\frac{1}{2\pi\gamma(D_T+\frac{D_A}{1+\gamma\tau_A})}}\exp[-\frac{v_t^2}{2\gamma(D_T+\frac{D_A}{1+\gamma\tau_A})}]$, which is the same as Eq. (10) involving the variance given in Eq. (11). However, for $\lambda \to \infty$, the variance is inversely related to λ, viz., $\sigma_v^2 \approx D_T\gamma + \frac{1}{\tau_A^2}\frac{D_A}{\lambda}$. The limiting cases just addressed above are applicable for both OUP and MOUP models. However, the results differ significantly for the variations in τ_A and γ. In the OUP bath, the active noise becomes uncorrelated in the limit $\tau_A \to 0$, as mentioned earlier, and therefore the distribution is of Boltzmannian type with an enhanced temperature $(D_T + D_A)\gamma$. On the contrary, it approaches the equilibrium distribution in this limit for the MOUP model. Now let us consider the limit $\gamma\tau_A \gg \lambda\tau_A \gg 1$. In the OUP bath, σ_v^2 can be approximated as $\sigma_v^2 \approx D_T\gamma + \frac{1}{\tau_A^2}\frac{D_A}{\lambda}$, which is similar to the liming case of $\lambda \to \infty$. Substituting D_A with $\frac{f_0^2}{\gamma^2}\tau_A$ for the MOUP bath leads to $\sigma_v^2 \approx T + \frac{1}{\lambda\tau_A}\frac{f_0^2}{\gamma^2}$, dictating $1/\tau_A$ dependence for a fixed value of f_0. Clearly, the effect of τ_A on velocity is different for the unconfined and confined particle.

Now we turn to the marginal distribution of x_t at the steady state. Taking the limit $t \to \infty$ in Eq. (C5), one gets the stationary PDF as

$$P_{\text{st}}(x_t) = \sqrt{\frac{1}{2\pi\sigma_x^2}}e^{-\frac{x_t^2}{2\sigma_x^2}}, \quad (17)$$

with $\sigma_x^2 = \frac{D_T}{\lambda} + \frac{D_A}{\lambda}\frac{1+\gamma\tau_A}{1+\gamma\tau_A+\gamma\lambda\tau_A^2}$. For a free particle ($\lambda \to 0$), the system cannot reach a steady state, as one can expect. In the large λ limit or for $\gamma\tau_A \gg \lambda\tau_A \gg 1$, $\sigma_x^2 \approx \frac{D_T}{\lambda} + \frac{1}{\tau_A}\frac{D_A}{\lambda^2}$, implying the inverse-dependence on λ. In particular, for the case where the active noise is dominant, i.e., $D_A \gg D_T$, the variance strongly depends on the stiffness, viz., $\sigma_x^2 \propto 1/\lambda^2$. In the OUP bath, σ_x^2 is inversely proportional to τ_A, but it is independent of τ_A in the case of MOUP bath, i.e., $\sigma_x^2 \approx T + \frac{f_0^2}{\lambda^2\gamma^2}$. For a very small persistence time ($\tau_A \to 0$), $\sigma_x^2 \approx \frac{D_T+D_A}{\lambda}$ in the OUP bath, corresponding here to a purely Gaussian white bath characterized by an enhanced diffusivity $D_T + D_A$. However, the active contribution vanishes in this limit for the MOUP model, and the system reaches near equilibrium. In the overdamped limit, i.e., for $\gamma\tau_A \gg 1$ and $\lambda\tau_A \gg 1$, one can recover the known result for the effective temperature in the OUP model as reported in Ref. [52], and it is given by $T_{\text{eff}} = \frac{\sigma_x^2}{\lambda} \approx D_T + \frac{D_A}{1+\lambda\tau_A}$.

Figure 2 shows the distributions of position and velocity at a large time. It is evident that the confinement keeps the particle near the origin, thus resulting the narrower distribution. Like the potential-free case, the effect of τ_A (or $1/\gamma$) is reverse in the two models. However, τ_A influences the dynamics more in the OUP model, while γ does the same in the MOUP model.

IV. WORK FLUCTUATIONS

Here we analyze the effect of active noise on work fluctuations of a passive particle in the underdamped limit. First, we compute the probability distribution function of work,

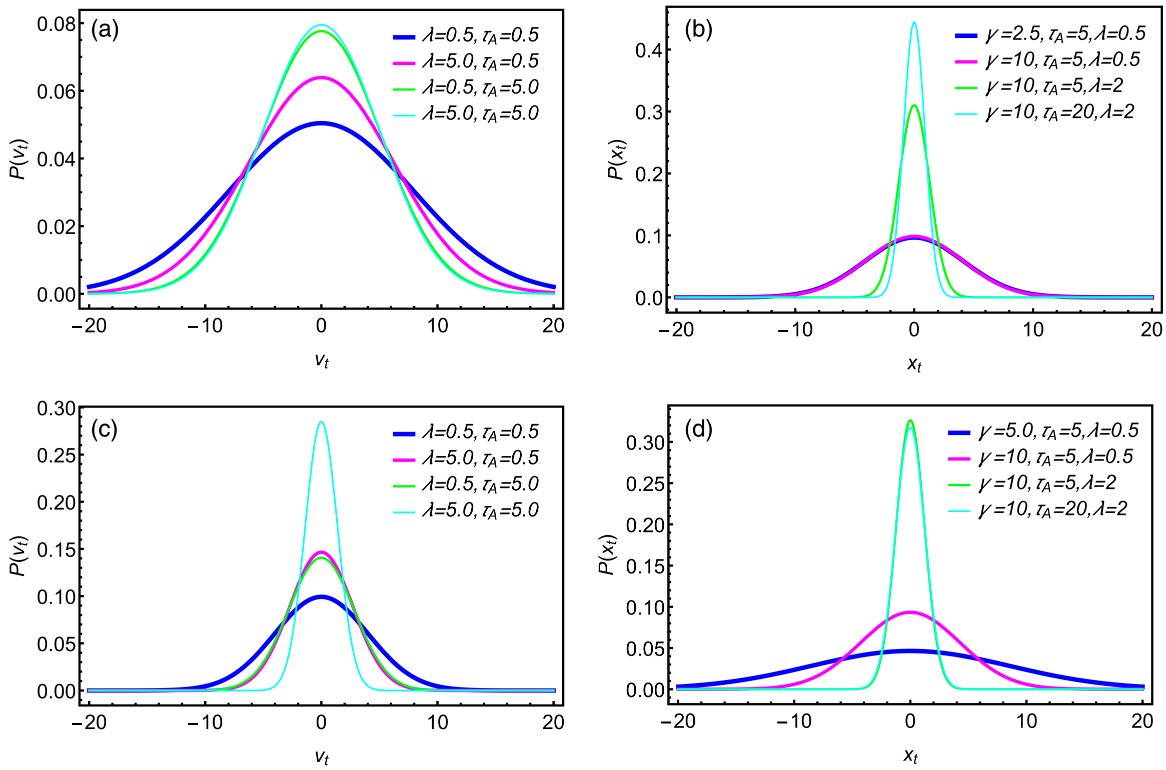

FIG. 2. Plots of the probability distribution functions (PDF) [Eqs. (C3) and (C5)] for a harmonically bound particle at time $t = 10$ for different values of parameters. The distributions of v_t and x_t for the OUP model are shown in panels (a, b), respectively, for fixed values of diffusivities $D_T = 1.0$, $D_A = 25$. Panels (c, d) show the PDFs of v_t and x_t in the MOUP bath considering $T = 1$, $f_0 = 25$. The values of parameter γ in panels (a, c) are $\gamma = 25.0$ and $\gamma = 5.0$, respectively.

considering a specific protocol for the performed work. Using the results, we look into the fluctuation theorem.

A. Probability distribution function of work *W*

Here we assume that the passive particle is confined in a harmonic potential with stiffness λ, and the center of the potential is pulled at a constant speed u for a time period t. Therefore, the particle experiences a time-dependent force $F(x,t) = \partial U(x,t)/\partial x$, where the potential is given by

$$U[x(t_1), t_1] = \frac{\lambda}{2}[x(t_1) - ut_1]^2. \tag{18}$$

Within an interval [0, t], the work performed on the particle can be expressed as [53]

$$W[x(t)] = \int_0^t \frac{\partial U[x(t_1), t_1]}{\partial t_1} dt_1 = \frac{\lambda}{2}u^2t^2 - \lambda u \int_0^t dt_1\, x(t_1). \tag{19}$$

So one can define the probability distribution function (PDF) of work as follows:

$$P(W) = \langle \delta\{W - W[x(t)]\}\rangle = \frac{1}{2\pi}\int_{-\infty}^{+\infty} d\alpha\, e^{i\alpha W}\langle e^{-i\alpha W[x(t)]}\rangle. \tag{20}$$

Here the angular bracket $\langle\cdots\rangle$ denotes the ensemble average over all possible trajectories of $x(t)$. After some mathematical steps, one can find the distribution $P(W)$, as detailed in Appendix D. The result [Eq. (D5)] is graphically illustrated over a range of parameters in Fig. 3. With time, the peak of the distribution shifts towards the larger values of W, implying that the performed work on average takes higher values if it is done for longer times, as anticipated. In the OUP bath, the distribution is more concentrated around the mean at shorter times, or for that matter, at any timescale in the underdamped regime compared to an overdamped case, considering that the particle has the same diffusivities for both cases. Note that a similar feature has been observed for the spatial distribution of a free particle in Fig. 1(b). On the contrary, the distribution comparatively spreads more in the low-friction (underdamped) limit for the MOUP model, as can be seen in Fig. 3(c). Like other cases, τ_A has similar role as $1/\gamma$, which is displayed in Figs. 3(b) and 3(d).

Now we analyze the result for work distribution at the stationary limit by taking $\gamma t \gg 1$, $\lambda t \gg 1$, and $t \gg \tau_A$. In this limit, one can approximate the average (mean) work as $\bar{W}(t) \approx u^2 t$, and the variance as

$$\begin{aligned}\sigma_W^2(t) &\approx 2D_T u^2 t + \frac{D_A u^2\left[1 - \gamma\tau_A + \lambda\gamma\tau_A^2\right]}{\gamma^2\lambda^2\tau_A^4 - \gamma^2\tau_A^2 + 2\gamma\lambda\tau_A^2 + 1} \\ &\quad \times \frac{1}{\gamma\lambda}[2\lambda\gamma^2\tau_A(\lambda\tau_A t + t) + 2\lambda\gamma t] \\ &\approx 2(D_T + D_A)u^2 t.\end{aligned}$$

The results in the stationary limit hold true for both OUP and MOUP models, and so we shall not specify the model further in the following discussion.

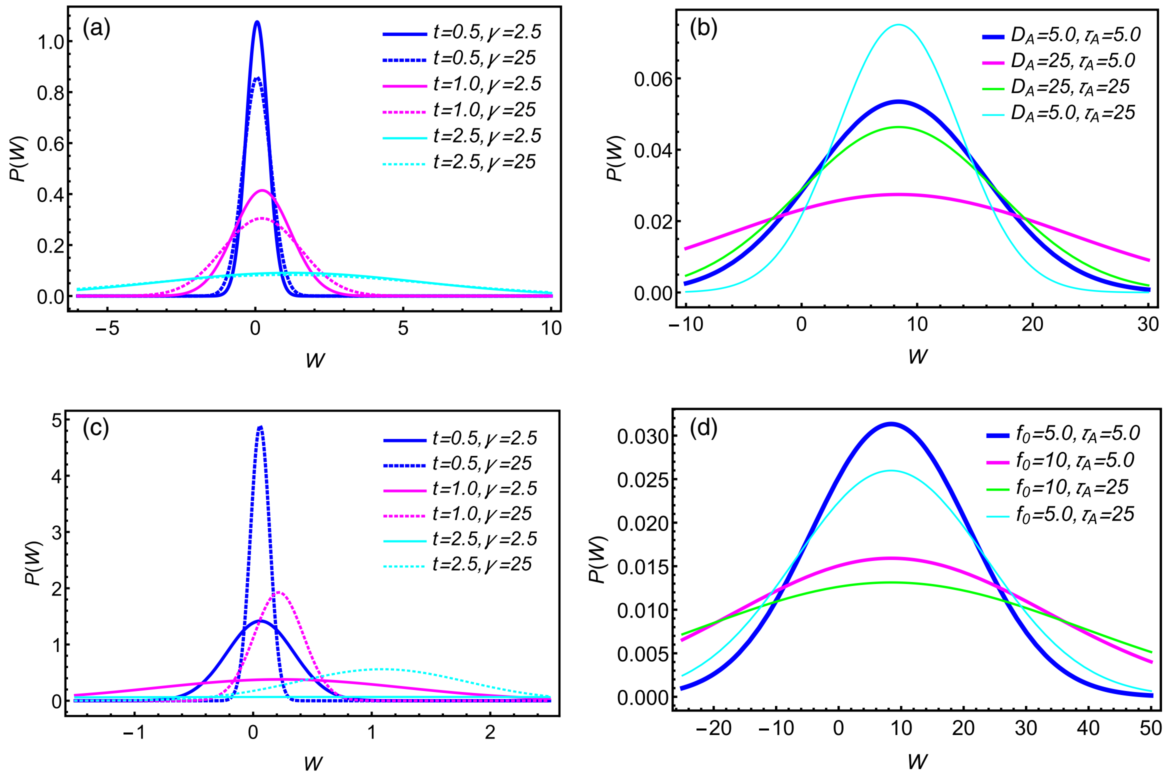

FIG. 3. The probability distribution function (PDF) of work [Eq. (D5)] is plotted as a function of work W performed on the particle trapped in a harmonic potential with stiffness $\lambda = 0.5$, and the trap-center is set in motion with a constant speed $u = 1$. In panels (a, c) the PDFs at different times are shown for the OUP and MOUP models, respectively taking the persistence time fixed at $\tau_A = 0.5$. In the OUP bath, we keep the values of diffusivities fixed at $D_T = 1.0$, $D_A = 25$, and the set $\{T = 1.0,\ f_0 = 25.0\}$ is taken for the MOUP model in panel (c). Panels (b, d) depict the distributions of work at time $t = 10$ for different values of parameters in the OUP and MOUP baths, respectively. In panel (b) we take $D_T = 1.0$, and in panel (d) the ambient temperature is fixed at $T = 1.0$.

Using the above mean and variance, the work distribution given in Eq. (D5) can be simplified to

$$P(W) = \sqrt{\frac{1}{4\pi(D_T + D_A)u^2 t}}\, e^{-\frac{(W-u^2 t)^2}{4(D_T+D_A)u^2 t}}, \tag{21}$$

which can also be obtained in the Gaussian white bath characterized by an elevated diffusivity $D_T + D_A$. Note that, in the stationary limit, the inertial effect dies out as $t \gg 1/\gamma$, and therefore, the distribution resembles the one in the overdamped case [54].

B. Work fluctuation theorem

A number of macroscopic properties can be extracted from the fluctuations of thermodynamic variables such as work at a trajectory level, and it is quantified with the application of fluctuation theorems (FTs). In the thermal bath, the distributions of positive and negative work are related via the work fluctuation theorem, viz. [55,56],

$$\frac{P(-W)}{P(W)} = e^{-\frac{W-\Delta\mathcal{F}}{k_B T}}. \tag{22}$$

For the protocol that we have employed in this paper to perform the work, there is no change of free energy $\mathcal{F}$, i.e., $\Delta\mathcal{F} = 0$. Also note that the potential has been rescaled by γ, and so alternatively, we can write D_T in place of thermal energy $k_B T$. Here Eq. (22) represents the conventional FT. Now, in a nonthermal bath, Eq. (22) is usually violated due to the presence of an additional noise, e.g., see Refs. [54,57,58]. But the system satisfies an equivalent relation at the steady state, viz.,

$$\frac{P(-W)}{P(W)} = e^{-\frac{W}{D_T+D_A}}, \tag{23}$$

with D_A being the diffusivity solely due to the additional noise. The above equation is referred to as the extended steady-state fluctuation theorem (ESSFT).

To validate the FT, we have plotted the ratio of PDFs of positive and negative work in Fig. 4. Notice that Eq. (22) is satisfied at a very shorter timescale. This is obvious as we have assumed that the system was initially in thermal equilibrium with the surroundings (before the introduction of active noise). As time passes, active fluctuations push the system out of equilibrium, and consequently, the system fails to obey Eq. (22). However, it attains a nonequilibrium steady state at long times, and at this condition, it obeys the ESSFT given in Eq. (23), as graphically shown in Fig. 4. This can be easily understood from the steady-state distribution given in Eq. (21), involving an effective temperature $D_T + D_A$. Not surprisingly, the FT is satisfied with the same temperature.

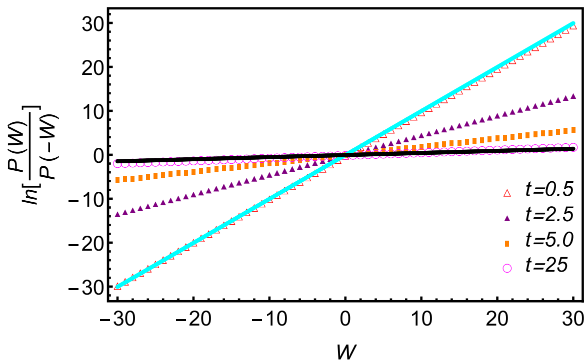

FIG. 4. Logarithmic plot of ratio of distributions for positive and negative work as a function of performed work. The curves with symbols are drawn using Eq. (D5) for different times. The two solid lines [cyan (light gray) and black] correspond to fluctuation theorems given by Eqs. (22) and (23), respectively. Other parameters are as follows: $D_T = 1$, $D_A = 20$, $\gamma = 2.5$, $\lambda = 0.5$, $\tau_A = 5$, $u = 1$.

V. CONCLUSION

In this paper, we have investigated the dynamics of an inertial particle in an active bath characterized by two types of Ornstein-Uhlenbeck (OU) processes. Two timescales, namely, inertial time and correlation time are found to be important and have almost similar effect on the dynamics. In the bath modeled by the usual OU process, the particle covers a shorter average distance if the motion is highly persistent. On the contrary, long-range correlations (or low dragging) cause the particle to travel longer distances if the bath is described by the modified Ornstein-Uhlenbeck process. Similar effects have been found on the work fluctuations. However, in the steady-state limit, the dynamical parameters become irrelevant, and the system follows the extended fluctuation theorem with an effective temperature.

Here we present a simple but effective formalism to deal with an underdamped particle in the presence of an active (extra) noise. This method can also be applied to obtain other dynamical quantities of inertial active particles such as mean-square speed and swim pressure. Apart from work fluctuations, one can employ this technique to explore several thermodynamic properties such as energy fluctuations, entropy productions, etc.

ACKNOWLEDGMENTS

The author acknowledges anonymous referees and Professor Rajarshi Chakrabarti for their useful comments. The project was funded by IIT Bombay through the institute postdoctoral fellowship.

APPENDIX A: CHARACTERISTIC FUNCTIONAL OF GAUSSIAN NOISE $\eta_A(t)$

As discussed earlier, the noise $\eta_A(t)$ can be expressed in terms of the Ornstein-Uhlenbeck process (OUP) as given in Eq. (2). The analytical solution for the OUP is known and well documented, e.g., see Ref. [59]. It can be represented as

$$\eta_A(t) = \eta_A(0)e^{-\frac{t}{\tau_A}} + \frac{1}{\tau_A}\int_0^t dt_1\, e^{-\frac{t-t_1}{\tau_A}}\xi(t_1), \tag{A1}$$

where $\eta_A(0)$ follows the initial distribution $P[\eta_A(0)]$, $P[\eta_A(0)] = \sqrt{\frac{\tau_A}{2\pi D_A}}\, e^{-\frac{\tau_A}{2D_A}\eta_A^2(0)}$. Here $\xi(t)$ is the white Gaussian noise and it has the following probability distribution functional: $\mathbb{P}[\xi] = e^{-\frac{1}{4D_A}\int_0^t dt_1 \xi^2(t_1)}$. By virtue of Eq. (A1), the characteristic functional of $\eta_A(t)$ can be expressed as

$$\langle e^{i\int_0^t dt_1\, p(t_1)\eta_A(t_1)}\rangle_{\eta_A} = \langle e^{i\eta_A(0)\int_0^t dt_1\, p(t_1)e^{-\frac{t_1}{\tau_A}}}\rangle_{\eta_A(0)} \times \langle e^{\frac{i}{\tau_A}\int_0^t dt_1\, p(t_1)\int_0^{t_1} dt_2\, e^{-\frac{t_1-t_2}{\tau_A}}\xi(t_2)}\rangle_\xi. \tag{A2}$$

Using the distributions of $\eta(0)$ and $\xi(t)$, one can derive the averages as follows:

$$\begin{aligned}
&\langle e^{i\eta_A(0)\int_0^t dt_1\, p(t_1)e^{-\frac{t_1}{\tau_A}}}\rangle_{\eta_A(0)}\\
&= \int d\eta_A(0)\, P[\eta_A(0)]e^{i\eta_A(0)\int_0^t dt_1\, p(t_1)e^{-\frac{t_1}{\tau_A}}}\\
&= \sqrt{\frac{\tau_A}{2\pi D_A}}\int d\eta_A(0)\, e^{-\frac{\tau_A}{2D_A}\eta_A^2(0)}e^{i\eta_A(0)\int_0^t dt_1\, p(t_1)e^{-\frac{t_1}{\tau_A}}}\\
&= e^{-\frac{D_A}{2\tau_A}\int_0^t dt_1\int_0^t dt_2\, p(t_1)e^{-\frac{t_1+t_2}{\tau_A}}p(t_2)},
\end{aligned} \tag{A3}$$

$$\begin{aligned}
&\langle e^{\frac{i}{\tau_A}\int_0^t dt_1\, p(t_1)\int_0^{t_1} dt_2\, e^{-\frac{t_1-t_2}{\tau_A}}\xi(t_2)}\rangle_\xi\\
&= \langle e^{\frac{i}{\tau_A}\int_0^t dt_2\,\xi(t_2)\int_0^t dt_1\, p(t_1)\Theta(t_1-t_2)\Theta(t-t_1)\,e^{-\frac{t_1-t_2}{\tau_A}}}\rangle_\xi\\
&= \int d\xi\, e^{-\frac{1}{4D_A}\int_0^t dt_1\xi^2(t_1)+\frac{i}{\tau_A}\int_0^t dt_2\,\xi(t_2)\int_0^t dt_1\, p(t_1)\Theta(t_1-t_2)\Theta(t-t_1)\,e^{-\frac{t_1-t_2}{\tau_A}}}\\
&= e^{-\frac{D_A}{\tau_A^2}\int_0^t dt_3\int_0^t dt_2\int_0^t dt_1\, p(t_1)p(t_2)\Theta(t_1-t_3)\Theta(t_2-t_3)\,e^{-\frac{t_2-t_3}{\tau_A}}\,e^{-\frac{t_1-t_3}{\tau_A}}}\\
&= e^{-\frac{D_A}{\tau_A^2}\int_0^{\min(t_1,t_2)} dt_3\, e^{\frac{2t_3}{\tau_A}}\int_0^t dt_2\int_0^t dt_1\, p(t_1)p(t_2)\,e^{-\frac{t_1+t_2}{\tau_A}}}\\
&= \exp\left[-\frac{D_A}{2\tau_A}\int_0^t dt_2\int_0^t dt_1\, p(t_1)p(t_2)\,e^{-\frac{t_1+t_2}{\tau_A}}\left(e^{\frac{2\min(t_1,t_2)}{\tau_A}}-1\right)\right]\\
&= \exp\left[-\frac{D_A}{2\tau_A}\int_0^t dt_2\int_0^t dt_1\, p(t_1)p(t_2)\left(e^{-\frac{|t_1-t_2|}{\tau_A}}-e^{-\frac{t_1+t_2}{\tau_A}}\right)\right].
\end{aligned} \tag{A4}$$

In the third steps of Eqs. (A3) and (A4), we have performed the standard Gaussian integration. Substituting the results of Eqs. (A3) and (A4) in Eq. (A2), one can obtain

$$\langle e^{i\int_0^t dt_1\, p(t_1)\eta_A(t_1)}\rangle_{\eta_A} = e^{-\frac{D_A}{2\tau_A}\int_0^t dt_1\int_0^t dt_2\, p(t_1)\, e^{-\frac{|t_1-t_2|}{\tau_A}}\, p(t_2)}, \qquad (A5)$$

which is the characteristic functional of noise $\eta_A(t)$ with the autocorrelation function $\langle\eta_A(t_1)\eta_A(t_2)\rangle = \frac{D_A}{\tau_A}e^{-\frac{|t_1-t_2|}{\tau_A}}$.

APPENDIX B: PROBABILITY DISTRIBUTION FUNCTIONAL $\mathbb{P}[x]$

For the reader's convenience, here we briefly discuss the path integration technique applied to our case. To start with, we write down the probability distribution functional of white noise $\eta_T(t)$ in Eq. (1), which is given by $\mathbb{P}[\eta_T] = e^{-\frac{1}{4D_T}\int_0^t dt_1 \eta_T^2(t_1)}$. With the help of Eq. (1), the functional can be rewritten in terms of path $x(t)$, and it reads

$$\mathbb{P}_0[x(t)] \sim e^{-\frac{1}{4D_T}\int_0^t dt_1[\frac{1}{\gamma}\ddot{x}(t)+\dot{x}(t)+\frac{U'[x(t),t]}{m\gamma}-\eta_A(t)]^2}. \qquad (B1)$$

Since $x(t)$ and $\eta_A(t)$ follow different trajectories, one needs to take into account the distribution for η_A as well. So the probability distribution functional for the whole process is

$$\mathbb{P}\{[x(t),\eta_A(t)]\} \sim e^{-\frac{1}{4D_T}\int_0^t dt_1[\frac{1}{\gamma}\ddot{x}(t)+\dot{x}(t)+\frac{U'(x(t),t)}{m\gamma}-\eta_A(t)]^2-\frac{1}{4D_T}\int_0^t dt_1[\tau_A\dot{\eta}_A(t)+\eta_A(t)]^2}, \qquad (B2)$$

where the exponent in the above equation corresponds to the stochastic action. Now one can express the propagator as a path integral of $\mathbb{P}[\{x,\eta_A\}]$ with respect to $x(t)$ and $\eta_A(t)$ [60], and it reads

$$P(x_t, v_t, t|x_0, v_0, 0) = \int_{x(0)=x_0,\, v(0)=v_0}^{x(t)=x_t,\, v(t)=v_t} \mathcal{D}x\,\mathbb{P}[x], \qquad (B3)$$

where

$$\mathbb{P}[x] = \int \eta_{At}\int \eta_{A0}\, P(\eta_{A0})\int_{\eta_A(0)=\eta_{A0}}^{\eta_A(t)=\eta_{At}} \mathcal{D}\eta_A\,\mathbb{P}\{[x(t),\eta_A(t)]\}, \qquad (B4)$$

with $P(\eta_{A0})$ being the initial distribution of $\eta_A(t)$. Without the noise $\eta_A(t)$, one can employ semiclassical approximations for the path integration to get exact result [60,61]. However, a more convenient way to treat the problem where an extra noise $\eta_A(t)$ is involved is the phase-space path integration (PSPI) technique. Here one first finds the characteristic functional of the white noise which can be computed as follows:

$$\begin{aligned}\langle e^{i\int_0^t dt_1\, p(t_1)\eta_T(t_1)}\rangle_{\eta_T} &= \int \mathcal{D}\eta_T\, e^{i\int_0^t dt_1\, p(t_1)\eta_T(t_1)}\mathbb{P}[\eta_T]\\ &= \int \mathcal{D}\eta_T\, e^{-\frac{1}{4D_T}\int_0^t dt_1\eta_T^2(t_1)} e^{i\int_0^t dt_1\, p(t_1)\eta_T(t_1)}\\ &= e^{-D_T\int_0^t dt_1 p^2(t_1)}. \qquad (B5)\end{aligned}$$

Now we can perform inverse Fourier transform of the above, and it yields

$$\mathbb{P}[\eta_T] = \int \mathcal{D}p e^{-D_T\int_0^t dt_1 p^2(t_1) - i\int_0^t dt_1\, p(t_1)\eta_T(t_1)}. \qquad (B6)$$

Substituting η_T by using Eq. (1), one can obtain Eq. (5b), and finally, doing the ensemble average over all possible paths of $\eta_A(t)$, we arrive at Eq. (5c) which is equivalent to Eq. (B4). So the propagator is $P(x_t, v_t, t; x_0, v_0, 0) = \int_{x(0)=x_0,\, v(0)=v_0}^{x(t)=x_t,\, v(t)=v_t}\mathcal{D}x\,\mathbb{P}[x]$, as given by Eq. (6). The reader is referred to Refs. [36,51] for detailed discussions on this topic.

APPENDIX C: PROBABILITY DISTRIBUTION FUNCTION (PDF), $P(x_t, v_t, t)$

The details of the PDFs for two cases (free particle and harmonically confined particle) studied in Sec. III of this article are given below.

1. Free particle, $U(x) = 0$

In Sec. III A, the PDF has the form of Eq. (9) with $\mathbb{X}$ being the column matrix, and its transpose, $\mathbb{X}^T = (x_t, v_t)$. The inverse of matrix $\mathbb{C}_f$ is given by

$$\mathbb{C}_f^{-1} = \begin{bmatrix}\mathbb{C}_{xx}^{-1} & \mathbb{C}_{xv}^{-1}\\ \mathbb{C}_{vx}^{-1} & \mathbb{C}_{vv}^{-1}\end{bmatrix}, \qquad (C1)$$

where

$$\begin{aligned}\mathbb{C}_{xx}^{-1} &= \frac{1}{\mathbb{C}_0}\big[\gamma^2 D_T(\gamma^2\tau_A^2-1)^2 e^{2t(\gamma+\frac{1}{\tau_A})} - 2\gamma^3 D_A\tau_A(\gamma^2\tau_A^2-1)e^{\gamma t+\frac{t}{\tau_A}} + \gamma^2 D_A(\gamma^2\tau_A^2-1)(\gamma\tau_A+1)e^{\frac{2t}{\tau_A}}\\ &\quad + \gamma^2 D_A(\gamma\tau_A-1)(\gamma^2\tau_A^2-1)e^{2t(\gamma+\frac{1}{\tau_A})}\big],\\ \mathbb{C}_{xv}^{-1} = \mathbb{C}_{vx}^{-1} &= \frac{1}{\mathbb{C}_0}\{\gamma(\gamma^2\tau_A^2-1)(\gamma\tau_A+1)e^{t(\gamma+\frac{2}{\tau_A})}[(\gamma\tau_A-1)(D_T+D_A)-D_A] - \gamma D_T(\gamma^2\tau_A^2-1)^2\\ &\quad\times e^{2t(\gamma+\frac{1}{\tau_A})} - \gamma^3 D_A\tau_A^2(\gamma^2\tau_A^2-1)e^{\gamma t+\frac{t}{\tau_A}} + \gamma^2 D_A\tau_A(\gamma^2\tau_A^2-1)(\gamma\tau_A+1)e^{2\gamma t+\frac{t}{\tau_A}} - \gamma^2 D_A\tau_A\\ &\quad\times (\gamma^2\tau_A^2-1)e^{\gamma t+\frac{t}{\tau_A}} - \gamma D_A(\gamma^2\tau_A^2-1)^2 e^{2t(\gamma+\frac{1}{\tau_A})} + \gamma D_A(\gamma^2\tau_A^2-1)(\gamma\tau_A+1)e^{\frac{2t}{\tau_A}}\},\end{aligned}$$

$$\mathbb{C}_{vv}^{-1} = \frac{1}{\mathbb{C}_0}\{2(\gamma^2\tau_A^2-1)(\gamma\tau_A+1)e^{t(\gamma+\frac{2}{\tau_A})}[(\gamma\tau_A-1)(D_T+D_A)-D_A]+2D_T(\gamma^2\tau_A^2-1)^2(\gamma t-1)$$
$$\times\ e^{2t(\gamma+\frac{1}{\tau_A})}+2\gamma^2D_A\tau_A^2(\gamma^2\tau_A^2-1)(\gamma\tau_A+1)e^{2\gamma t+\frac{t}{\tau_A}}-2\gamma^2D_A\tau_A^2(\gamma^2\tau_A^2-1)e^{\gamma t+\frac{t}{\tau_A}}+D_A(\gamma^2\tau_A^2-1)$$
$$\times\ (\gamma\tau_A+1)e^{\frac{2t}{\tau}}+D_A(\gamma\tau_A-1)(\gamma^2\tau_A^2-1)e^{2t(\gamma+\frac{1}{\tau_A})}[-2\gamma\tau_A(\gamma\tau_A+2)+2\gamma t(\gamma\tau_A+1)-3]\}$$

and

$$\mathbb{C}_0 = -\gamma\big((\gamma\tau_A+1)^2e^{\frac{2t}{\tau_A}}\big(D_T^2(\gamma\tau_A-1)^2-D_TD_A(\gamma\tau_A-1)(-2\gamma\tau_A+2\gamma t+5)+D_A^2$$
$$\times\ \{\gamma[3\gamma\tau_A^2-2\tau(\gamma t+3)+2t]+4\}\big)+(\gamma\tau_A-1)^2e^{2t(\gamma+\frac{1}{\tau_A})}\{D_TD_A(\gamma\tau_A+1)[2\gamma\tau_A(\gamma\tau_A+3)-2\gamma t$$
$$\times\ (\gamma\tau_A+2)+7]-D_T^2(2\gamma t-3)(\gamma\tau_A+1)^2+D_A^2[3\gamma\tau_A(\gamma\tau_A+2)-2\gamma t(\gamma\tau_A+1)+4]\}+2\gamma^2D_A\tau_A$$
$$\times\ e^{t(\gamma+\frac{1}{\tau_A})}[D_T(\gamma^2\tau_A^2-1)(2t+3\tau_A)+2D_A(\gamma^2\tau_A^2t-2\tau_A-t)]-2\gamma D_A\tau_A(\gamma^2\tau^2-1)e^{t/\tau}[(\gamma\tau_A-1)$$
$$\times\ (D_T+2D_A)+D_A]-2\gamma D_A\tau_A(\gamma^2\tau_A^2-1)e^{t(2\gamma+\frac{1}{\tau_A})}[D_T(\gamma\tau_A+1)^2+2\gamma D_A\tau_A+D_A]-2(\gamma^2\tau_A^2-1)$$
$$\times\ e^{t(\gamma+\frac{2}{\tau_A})}[(\gamma\tau_A-1)(D_T+D_A)-D_A][(\gamma\tau_A+1)(2D_T+D_A)+D_A]+\gamma^2D_A^2\tau_A^2(\gamma\tau_A-1)^2$$
$$+\gamma^2D_A^2\tau_A^2(\gamma\tau_A+1)^2e^{2\gamma t}+2\gamma^2D_A^2\tau_A^2(\gamma^2\tau_A^2-1)e^{\gamma t}\big).$$

2. In a harmonic potential, $U(x) = \frac{\lambda}{2}x^2$

The distribution of velocity can be obtained after integrating the propagator given in Eq. (15) of Sec. III B over the initial and final positions and initial velocity, as follows:

$$P(v_t,t) = \int dx_t \int dv_0 \int dx_0 P(x_t,v_t,t|x_0,v_0,0)P_0(x_0,v_0)$$
$$= \int dx_t \int dv_0 \int dx_0 \int dp_t \int dp_0 e^{-D_T\int_0^t dt_1 p^2(t_1)}\langle e^{i\int_0^t dt_1\, p(t_1)\eta_A(t_1)}\rangle_{\eta_A} P_0(x_0,v_0)$$
$$\times\ e^{-\frac{i}{\gamma}[v_tp(t)-v_0p(0)]-ix_t[p(t)-\frac{1}{\gamma}\dot{p}(t)]+ix_0[p(0)-\frac{1}{\gamma}\dot{p}(0)]}, \quad \text{(C2)}$$

where $P_0(x_0,v_0)$ is the initial distribution of both position and velocity of the particle. Here we consider that the initial velocity has the Boltzmann distribution, and the particle was initially at position $x_0=0$, i.e., $P_0(x_0,v_0)=\delta(x_0)\sqrt{\frac{1}{2\pi\gamma D_T}}e^{-\frac{v_0^2}{2\gamma D_T}}$. Taking initial conditions into account, Eq. (C2) can be computed analytically, and it reads

$$P(v_t,t) = \sqrt{\frac{1}{2\pi\sigma_v^2(t)}}e^{-\frac{v_t^2}{2\sigma_v^2(t)}}, \quad \text{(C3)}$$

with

$$\sigma_v^2(t) = \frac{\gamma\, e^{-t(\frac{3\gamma}{2}+\frac{1}{\tau_A})}}{2\Gamma^2(-\gamma\tau_A+\Gamma\tau_A-2)(-\gamma\tau_A+\Gamma\tau_A+2)[\tau_A(\gamma+\Gamma)-2][\tau_A(\gamma+\Gamma)+2]}\Bigg[-32\gamma\Gamma D_A\tau_Ae^{\gamma t}\sinh\left(\frac{\Gamma t}{2}\right)$$
$$\times\ [\gamma(\gamma\tau_A+2)-\Gamma^2\tau_A]+64\gamma\Gamma^2D_A\tau_Ae^{\gamma t}\cosh\left(\frac{\Gamma t}{2}\right)+2\Gamma^2(-\gamma\tau_A+\Gamma\tau_A+2)[\tau_A(\gamma+\Gamma)-2]e^{t(\frac{1}{\tau_A}+\frac{3\gamma}{2})}$$
$$\times\ \{D_T(-\gamma\tau_A+\Gamma\tau_A-2)[\tau_A(\gamma+\Gamma)+2]-4D_A\}-(\gamma\tau_A-\Gamma\tau_A+2)[\tau_A(\gamma+\Gamma)+2]e^{t(\frac{1}{\tau_A}+\frac{\gamma}{2})}$$
$$\times\ (\cosh(\Gamma t)\{4\gamma D_A[\gamma(2-\gamma\tau_A)+\Gamma^2\tau_A]+(\Gamma-\gamma)(\gamma+\Gamma)D_T(-\gamma\tau_A+\Gamma\tau_A+2)[\tau_A(\gamma+\Gamma)-2]\}$$
$$-8\gamma\Gamma D_A\sinh(\Gamma t))+(\gamma-\Gamma)(\gamma+\Gamma)[\tau_A(\gamma+\Gamma)+2](\gamma\tau_A-\Gamma\tau_A+2)e^{t(\frac{1}{\tau_A}+\frac{\gamma}{2})}[\tau_A^2(\gamma-\Gamma)(\gamma+\Gamma)D_T$$
$$-4\gamma\tau_A(D_A+D_T)+8D_A+4D_T]\Bigg],$$

where $\Gamma=\sqrt{\gamma(\gamma-4\lambda)}$. The distribution of displacement can be expressed as

$$P(x_t,t) = \int dv_t \int dv_0 \int dx_0 P(x_t,v_t,t|x_0,v_0,0)P_0(x_0,v_0)$$
$$= \int dv_t \int dv_0 \int dx_0 \int dp_t \int dp_0 e^{-D_T\int_0^t dt_1 p^2(t_1)}\langle e^{i\int_0^t dt_1\, p(t_1)\eta_A(t_1)}\rangle_{\eta_A} P_0(x_0,v_0)$$
$$\times\ e^{-\frac{i}{\gamma}[v_tp(t)-v_0p(0)]-ix_t[p(t)-\frac{1}{\gamma}\dot{p}(t)]+ix_0[p(0)-\frac{1}{\gamma}\dot{p}(0)]}, \quad \text{(C4)}$$

and the integration over the variables leads to

$$P(x_t, t) = \sqrt{\frac{1}{2\pi\sigma_x^2(t)}}e^{-\frac{x_t^2}{2\sigma_x^2(t)}}, \tag{C5}$$

with

$$\begin{aligned}
\sigma_x^2(t) = &\frac{2\gamma\, e^{-\gamma t}}{\Gamma^2(\gamma-\Gamma)(\gamma+\Gamma)(\gamma\tau_A-\Gamma\tau_A-2)(\gamma\tau_A-\Gamma\tau_A+2)[\tau_A(\gamma+\Gamma)-2][\tau_A(\gamma+\Gamma)+2]} \\
&\times \Bigg(2\Gamma^2 e^{\gamma t}(-\gamma\tau_A+\Gamma\tau_A+2)[\tau_A(\gamma+\Gamma)-2]\big[\tau_A^2(\Gamma-\gamma)(\gamma+\Gamma)D_T-4\gamma\tau_A(D_A+D_T)-4(D_A+D_T)\big] \\
&-16\gamma\Gamma^2 D_A\tau_A^3(\gamma-\Gamma)(\gamma+\Gamma)\cosh\left(\frac{\Gamma t}{2}\right)e^{\frac{1}{2}t(\gamma-\frac{2}{\tau_A})}-\cosh(\Gamma t)(-\gamma\tau_A+\Gamma\tau_A-2)[\tau_A(\gamma+\Gamma)+2] \\
&\times\{4\gamma D_A[\tau_A(\gamma^2+\Gamma^2)-2\gamma]+(\gamma^2+\Gamma^2)D_T(-\gamma\tau_A+\Gamma\tau_A+2)[\tau_A(\gamma+\Gamma)-2]\}-2\gamma\Gamma \\
&\times\Bigg\{8D_A\tau_A^2(\gamma-\Gamma)(\gamma+\Gamma)(\gamma\tau_A+2)\sinh\left(\frac{\Gamma t}{2}\right)e^{\frac{1}{2}t(\gamma-\frac{2}{\tau_A})}+\sinh(\Gamma t)[\tau_A(\gamma+\Gamma)+2](\gamma\tau_A-\Gamma\tau_A+2) \\
&\times\big[\tau_A^2(\gamma-\Gamma)(\gamma+\Gamma)D_T-4\gamma\tau_A(D_A+D_T)+4(D_A+D_T)\big]\Bigg\}-(\Gamma-\gamma)(\gamma+\Gamma)(-\gamma\tau_A+\Gamma\tau_A-2) \\
&\times[\tau_A(\gamma+\Gamma)+2]\{4D_A(\gamma\tau_A-2)+D_T(-\gamma\tau_A+\Gamma\tau_A+2)[\tau_A(\gamma+\Gamma)-2]\}\Bigg).
\end{aligned}$$

APPENDIX D: COMPUTATION OF $P(W)$

To compute Eq. (20), one needs to find the characteristic function of work which is given by

$$\begin{aligned}
\mathcal{C}_W(\alpha) &= \langle e^{-i\alpha W[x(t)]}\rangle \\
&= \int dx_f\int dx_0\int dv_f\int dv_0\int Dx\, e^{-i\alpha W[x(t)]}\,\mathbb{P}[x(t)]\,\mathcal{P}(x_0, v_0),
\end{aligned} \tag{D1}$$

where $\mathcal{P}(x_0, v_0)$ is initial probability distribution function of the particle. By aid of Eqs. (5c) and (18), one can write

$$\begin{aligned}
\mathbb{P}[x(t)] = &\int Dq\, e^{-iq_t\frac{v_t}{\gamma}-ix_t(q_t-\frac{\dot{q}_t}{\gamma})+iq_0\frac{v_0}{\gamma}+ix_0(q_0-\frac{\dot{q}_0}{\gamma})}\, e^{-D_T\int_0^t dt_1\, q(t_1)^2}\langle e^{i\int_0^t dt_1\, q(t_1)\eta_A(t_1)}\rangle_{\eta_A(t_1)} \\
&\times\, e^{i\lambda u\int_0^t dt_1\, t_1 q(t_1)}\, e^{-i\int_0^t dt_1\, x(t_1)[\frac{\ddot{q}(t_1)}{\gamma}-\dot{q}(t_1)+\lambda q(t_1)]}.
\end{aligned} \tag{D2}$$

Therefore, Eq. (D1) can be rewritten explicitly, using Eq. (D2), as

$$\begin{aligned}
\mathcal{C}_W(\alpha) = &\int dx_t\int dx_0\int dv_t\int dv_0\int Dx\int Dq\, e^{-iq_t\frac{v_t}{\gamma}-ix_t(q_t-\frac{\dot{q}_t}{\gamma})+iq_0\frac{v_0}{\gamma}+ix_0(q_0-\frac{\dot{q}_0}{\gamma})}\mathcal{P}(x_0, v_0) \\
&\times\, e^{-D_T\int_0^t dt_1\, q(t_1)^2}\langle e^{i\int_0^t dt_1\, q(t_1)\eta_A(t_1)}\rangle_{\eta_A(t_1)}\, e^{i\lambda u\int_0^t dt_1\, t_1 q(t_1)}\, e^{-i\alpha\frac{\lambda}{2}u^2t^2}\, e^{-i\int_0^t dt_1\, x(t_1)[\frac{\ddot{q}(t_1)}{\gamma}-\dot{q}(t_1)+\lambda q(t_1)-\alpha\lambda u]}.
\end{aligned} \tag{D3}$$

One can perform the path integration over $x(t)$, which yields a δ functional, viz.,

$$\int Dx e^{-i\int_0^t dt_1\, x(t_1)[\frac{\ddot{q}(t_1)}{\gamma}-\dot{q}(t_1)+\lambda q(t_1)-\alpha\lambda u]} = \delta\left[\frac{\ddot{q}(t_1)}{\gamma}-\dot{q}(t_1)+\lambda q(t_1)-\alpha\lambda u\right].$$

Further, the integration over v_t and x_t can be done easily, as follows: $\int dv_t e^{-iq_t\frac{v_t}{\gamma}} = \delta(\frac{q_t}{\gamma})$, which implies $q_t = 0$. $\int dx_t e^{-ix_t(q_t-\frac{\dot{q}_t}{\gamma})} = \delta(q_t - \frac{\dot{q}_t}{\gamma})$, which leads to, $\dot{q}_t = \gamma q_t = 0$. Taking all these results into consideration, we obtain

$$q(t_1) = \alpha u - \frac{\alpha u}{\theta}e^{-\frac{\gamma}{2}(t-t_1)}\sinh\left[\frac{\gamma\theta}{2}(t-t_1)\right] - \alpha u\, e^{-\frac{\gamma}{2}(t-t_1)}\cosh\left[\frac{\gamma\theta}{2}(t-t_1)\right],$$

where $\theta = \sqrt{1-\frac{4\lambda}{\gamma}} = \frac{\Gamma}{\gamma}$.$\mathcal{P}(x_0, v_0)$ can be taken as an equilibrium, Boltzmannian distribution, viz.,

$$\mathcal{P}(x_0, v_0) = \sqrt{\frac{\lambda}{2\pi D_T}}\, e^{-\frac{\lambda}{2D_T}x_0^2}\sqrt{\frac{1}{2\gamma\pi D_T}}\, e^{-\frac{1}{2\gamma D_T}v_0^2}.$$

Now one can easily perform the integration over x_0 and v_0 in Eq. (D3), and it reads

$$\int dx_0 \int dv_0 e^{iq_0\frac{v_0}{\gamma}+ix_0(q_0-\frac{\dot{q}_0}{\gamma})}\mathcal{P}(x_0, v_0) = e^{-\frac{D_T}{2\lambda}(q_0-\frac{\dot{q}_0}{\gamma})^2-\frac{D_T}{2\gamma}q_0^2}.$$

Therefore, Eq. (D3) can be recast as

$$\mathcal{C}_W(\alpha) = e^{-D_T\int_0^t dt_1\, q(t_1)^2}\langle e^{i\int_0^t dt_1\, q(t_1)\eta_A(t_1)}\rangle_{\eta_A(t_1)}\, e^{i\lambda u\int_0^t dt_1\, t_1 q(t_1)}\, e^{-i\alpha\frac{\lambda}{2}u^2t^2}\, e^{-\frac{D_T}{2\lambda}(q_0-\frac{\dot{q}_0}{\gamma})^2-\frac{D_T}{2\gamma}q_0^2}. \tag{D4}$$

The average over $\eta_A(t_1)$ can be calculated using Eq. (4). Finally, by virtue of Eq. (D4) and Eq. (20), the distribution of work can be expressed as

$$P(W) = \frac{1}{2\pi}\int_{-\infty}^{+\infty} d\alpha\, e^{i\alpha[W-\bar{W}(t)]-\alpha^2\frac{\sigma_W^2(t)}{2}} = \sqrt{\frac{1}{2\pi\sigma_W^2(t)}}\, e^{-\frac{(W-\bar{W})^2}{2\sigma_W^2(t)}}, \tag{D5}$$

where the mean of the work is given by

$$\begin{aligned}\bar{W}(t) &= \frac{\lambda}{2}u^2t^2 - \lambda u\int_0^t dt_1\, t_1\left\{u - \frac{u}{\theta}e^{-\frac{\gamma}{2}(t-t_1)}\sinh\left[\frac{\gamma\theta}{2}(t-t_1)\right] - u\, e^{-\frac{\gamma}{2}(t-t_1)}\cosh\left[\frac{\gamma\theta}{2}(t-t_1)\right]\right\}\\ &= u^2\left[t + \frac{1}{\gamma} - \frac{1}{\lambda} + \left(\frac{1}{\lambda}-\frac{1}{\gamma}\right)e^{-\frac{\gamma}{2}t}\cosh\left(\frac{\gamma}{2}\theta t\right) + \left(\frac{1}{\theta\lambda}-\frac{3}{\theta\gamma}\right)e^{-\frac{\gamma}{2}t}\sinh\left(\frac{\gamma}{2}\theta t\right)\right],\end{aligned} \tag{D6}$$

and the variance of the work can be written as

$$\begin{aligned}\sigma_W^2(t) &= 2D_T\int_0^t dt_1\left\{u - \frac{u}{\theta}e^{-\frac{\gamma}{2}(t-t_1)}\sinh\left[\frac{\gamma\theta}{2}(t-t_1)\right] - u\, e^{-\frac{\gamma}{2}(t-t_1)}\cosh\left[\frac{\gamma\theta}{2}(t-t_1)\right]\right\}^2\\ &\quad + \frac{D_A}{\tau_A}\int_0^t\int_0^t dt_1\, dt_2\left\{u - \frac{u}{\theta}e^{-\frac{\gamma}{2}(t-t_2)}\sinh\left[\frac{\gamma\theta}{2}(t-t_2)\right] - u\, e^{-\frac{\gamma}{2}(t-t_2)}\cosh\left[\frac{\gamma\theta}{2}(t-t_2)\right]\right\}e^{-\frac{|t_1-t_2|}{\tau_A}}\\ &\quad \times\left\{u - \frac{u}{\theta}e^{-\frac{\gamma}{2}(t-t_1)}\sinh\left[\frac{\gamma\theta}{2}(t-t_1)\right] - u\, e^{-\frac{\gamma}{2}(t-t_1)}\cosh\left[\frac{\gamma\theta}{2}(t-t_1)\right]\right\} + \frac{D_T}{\gamma}\left[u - ue^{-\frac{\gamma}{2}t}\cosh\left(\frac{\gamma}{2}\theta t\right)\right.\\ &\quad \left.-\frac{u}{\theta}e^{-\frac{\gamma}{2}t}\sinh\left(\frac{\gamma}{2}\theta t\right)\right]^2 + \frac{D_T}{\lambda}\left[u - ue^{-\frac{\gamma}{2}t}\cosh\left(\frac{\gamma}{2}\theta t\right) - \frac{u}{\theta}e^{-\frac{\gamma}{2}t}\sinh\left(\frac{\gamma}{2}\theta t\right) + \frac{u}{2\theta}e^{-\frac{\gamma}{2}t}\sinh\left(\frac{\gamma}{2}\theta t\right)\right.\\ &\quad \left.-\frac{u\theta}{2}e^{-\frac{\gamma}{2}t}\sinh\left(\frac{\gamma}{2}\theta t\right)\right]^2\\ &= 2D_Tu^2\left[t + \frac{1}{\gamma} - \frac{1}{\lambda} + \left(\frac{1}{\lambda}-\frac{1}{\gamma}\right)e^{-\frac{\gamma}{2}t}\cosh\left(\frac{\gamma}{2}\theta t\right) + \left(\frac{1}{\theta\lambda}-\frac{3}{\theta\gamma}\right)e^{-\frac{\gamma}{2}t}\sinh\left(\frac{\gamma}{2}\theta t\right)\right]\\ &\quad + \frac{D_Au^2}{\gamma^2\lambda^2\tau_A^4-\gamma^2\tau_A^2+2\gamma\lambda\tau_A^2+1}\left[2e^{-\frac{t}{\tau_A}}\gamma\lambda\tau_A^3\left(1+\gamma\tau_A+\lambda\gamma\tau_A^2\right) + \frac{2\lambda e^{-\gamma t}}{\gamma^2\theta^2}(2-\gamma\tau_A)\left(1+\gamma\tau_A+\lambda\gamma\tau_A^2\right)\right.\\ &\quad + \frac{e^{-\gamma t(1+\theta)}}{2\lambda\theta^2}\left(1+\gamma\tau_A+\lambda\gamma\tau_A^2\right)\left[\frac{2\lambda^2}{\gamma}\tau_A + \theta\tau_A(2\lambda-\gamma) + \frac{\lambda}{\gamma}(3-\theta) - 4\lambda\tau_A + \gamma\tau_A + \theta - 1\right]\\ &\quad + \frac{e^{-\gamma t(1-\theta)}}{2\lambda\theta^2}\left(1+\gamma\tau_A+\lambda\gamma\tau_A^2\right)\left[\frac{2\lambda^2}{\gamma}\tau_A - \theta\tau_A(2\lambda-\gamma) + \frac{\lambda}{\gamma}(3+\theta) - 4\lambda\tau_A + \gamma\tau_A - \theta - 1\right]\\ &\quad + \frac{\tau_A}{\theta}e^{-\frac{(1-\theta)}{2}\gamma t-\frac{T}{\tau_A}}\left(\theta - \theta\gamma^2\tau_A^2 - \lambda\gamma\tau_A^2 - \lambda\gamma^2\tau_A^3 + 2\lambda^2\gamma\tau_A^3\right) + \frac{\tau_A}{\theta}\left(\theta - \theta\gamma^2\tau_A^2 + \lambda\gamma\tau_A^2 + \lambda\gamma^2\tau_A^3 - 2\lambda^2\gamma\tau_A^3\right)\\ &\quad \times e^{-\frac{(1+\theta)}{2}\gamma t-\frac{T}{\tau_A}} + \frac{1}{\gamma\lambda\theta}\left(1+\gamma\tau_A+\lambda\gamma\tau_A^2\right)\{\gamma[\gamma\tau_A(\lambda\tau_A-2)+\lambda\tau_A(5-2\lambda\tau_A)+2]-4\lambda\}\\ &\quad \times\left[e^{-\frac{(1-\theta)}{2}\gamma t} - e^{-\frac{(1+\theta)}{2}\gamma t}\right] + \frac{1}{\gamma\lambda}(\lambda + \gamma^2\tau_A\{2\lambda[-\tau_A(\lambda\tau_A+2)+\lambda\tau_At+t]-3\} + \gamma(2\lambda t-3))\\ &\quad \times\left(1-\gamma\tau_A+\lambda\gamma\tau_A^2\right) + \frac{1}{\lambda}\left[e^{-\frac{(1-\theta)}{2}\gamma t} + e^{-\frac{(1+\theta)}{2}\gamma t}\right]\left(1+\gamma\tau_A+\lambda\gamma\tau_A^2\right)[\gamma\tau_A(\lambda\tau_A-2)+\lambda\tau_A+2]\\ &\quad \left.-\tau_A\left[e^{-\frac{(1-\theta)}{2}\gamma t-\frac{t}{\tau_A}} + e^{-\frac{(1+\theta)}{2}\gamma t-\frac{t}{\tau_A}}\right](\gamma\tau_A+1)[\gamma\tau_A(\lambda\tau_A-1)+1]\right].\end{aligned} \tag{D7}$$

[1] D. B. Kearns, Nat. Rev. Microbiol. **8**, 634 (2010).
[2] T. Sanchez, D. T. Chen, S. J. DeCamp, M. Heymann, and Z. Dogic, Nature (London) **491**, 431 (2012).
[3] D. Selmeczi, L. Li, L. I. Pedersen, S. Nrrelykke, P. H. Hagedorn, S. Mosler, N. B. Larsen, E. C. Cox, and H. Flyvbjerg, Eur. Phys. J. Spec. Top. **157**, 1 (2008).
[4] T. Vicsek and A. Zafeiris, Phys. Rep. **517**, 71 (2012).
[5] J. Toner, Y. Tu, and S. Ramaswamy, Ann. Phys. **318**, 170 (2005).
[6] P. Romanczuk, M. Bär, W. Ebeling, B. Lindner, and L. Schimansky-Geier, Eur. Phys. J.: Spec. Top. **202**, 1 (2012).
[7] J. Stenhammar, A. Tiribocchi, R. J. Allen, D. Marenduzzo, and M. E. Cates, Phys. Rev. Lett. **111**, 145702 (2013).
[8] S. Das, S. Ghosh, and R. Chelakkot, Phys. Rev. E **102**, 032619 (2020).
[9] L. L. Bonilla, Phys. Rev. E **100**, 022601 (2019).
[10] D. Martin, J. O'Byrne, M. E. Cates, É. Fodor, C. Nardini, J. Tailleur, and F. van Wijland, Phys. Rev. E **103**, 032607 (2021).
[11] E. Woillez, Y. Kafri, and N. S. Gov, Phys. Rev. Lett. **124**, 118002 (2020).
[12] D. Martin and T. A. de Pirey, J. Stat. Mech. (2021) 043205.
[13] A. P. Solon, M. E. Cates, and J. Tailleur, Eur. Phys. J.: Spec. Top. **224**, 1231 (2015).
[14] M. E. Cates and J. Tailleur, Europhys. Lett. **101**, 20010 (2013).
[15] K. Malakar, V. Jemseena, A. Kundu, K. V. Kumar, S. Sabhapandit, S. N. Majumdar, S. Redner, and A. Dhar, J. Stat. Mech. (2018) 043215.
[16] D. Klotsa, Soft Matter **15**, 8946 (2019).
[17] S. Wang and A. Ardekani, Phys. Fluids **24**, 101902 (2012).
[18] G. Li, A. Ostace, and A. M. Ardekani, Phys. Rev. E **94**, 053104 (2016).
[19] H. Mukundarajan, T. C. Bardon, D. H. Kim, and M. Prakash, J. Exp. Biol. **219**, 752 (2016).
[20] T. Dombrowski, S. K. Jones, G. Katsikis, A. P. S. Bhalla, B. E. Griffith, and D. Klotsa, Phys. Rev. Fluids **4**, 021101(R) (2019).
[21] H. L. Devereux, C. R. Twomey, M. S. Turner, and S. Thutupalli, J. R. Soc. Interface **18**, 20210114 (2021).
[22] J. Rabault, R. A. Fauli, and A. Carlson, Phys. Rev. Lett. **122**, 024501 (2019).
[23] C. Scholz, M. Engel, and T. Pöschel, Nat. Commun. **9**, 931 (2018).
[24] C. Scholz, S. Jahanshahi, A. Ldov, and H. Löwen, Nat. Commun. **9**, 5156 (2018).
[25] L. Giomi, N. Hawley-Weld, and L. Mahadevan, Proc. R. Soc. A **469**, 20120637 (2013).
[26] H. Löwen, J. Chem. Phys. **152**, 040901 (2020).
[27] L. Caprini and U. Marini Bettolo Marconi, J. Chem. Phys. **154**, 024902 (2021).
[28] L. L. Gutierrez-Martinez and M. Sandoval, J. Chem. Phys. **153**, 044906 (2020).
[29] L. Caprini and U. M. B. Marconi, Soft Matter **17**, 4109 (2021).
[30] S. Mandal, B. Liebchen, and H. Löwen, Phys. Rev. Lett. **123**, 228001 (2019).
[31] M. Sandoval, Phys. Rev. E **101**, 012606 (2020).
[32] B.-Q. Ai and F.-G. Li, Soft Matter **13**, 2536 (2017).
[33] A. Argun, A.-R. Moradi, E. Pinçe, G. B. Bagci, A. Imparato, and G. Volpe, Phys. Rev. E **94**, 062150 (2016).
[34] C. Maggi, M. Paoluzzi, N. Pellicciotta, A. Lepore, L. Angelani, and R. Di Leonardo, Phys. Rev. Lett. **113**, 238303 (2014).
[35] S. Krishnamurthy, S. Ghosh, D. Chatterji, R. Ganapathy, and A. Sood, Nat. Phys. **12**, 1134 (2016).
[36] K. Goswami and K. L. Sebastian, J. Stat. Mech. (2019) 083501.
[37] K. Goswami, Ph.D. thesis, Indian Institute of Science, 2020.
[38] M. E. Cates and J. Tailleur, Annu. Rev. Condens. Matter Phys. **6**, 219 (2015).
[39] C. Bechinger, R. Di Leonardo, H. Löwen, C. Reichhardt, G. Volpe, and G. Volpe, Rev. Mod. Phys. **88**, 045006 (2016).
[40] S. Chaki and R. Chakrabarti, Physica A **511**, 302 (2018).
[41] K. Goswami, Physica A **566**, 125609 (2021).
[42] T. Taniguchi and E. Cohen, J. Stat. Phys. **130**, 1 (2008).
[43] J. Jiménez-Aquino and N. Sánchez-Salas, Physica A **509**, 12 (2018).
[44] P. V. Paraguassú, R. Aquino, and W. A. Morgado, arXiv:2102.09115.
[45] V. Holubec and R. Marathe, Phys. Rev. E **102**, 060101(R) (2020).
[46] S. Shankar and M. C. Marchetti, Phys. Rev. E **98**, 020604(R) (2018).
[47] E. Fodor, C. Nardini, M. E. Cates, J. Tailleur, P. Visco, and F. van Wijland, Phys. Rev. Lett. **117**, 038103 (2016).
[48] G. H. P. Nguyen, R. Wittmann, and H. Löwen, J. Condens. Matter Phys. **34**, 035101 (2021).
[49] N. G. Van Kampen, *Stochastic Processes in Physics and Chemistry*, Vol. 1 (Elsevier, Amsterdam, 1992).
[50] A. Kamenev, *Field Theory of Non-Equilibrium Systems* (Cambridge University Press, Cambridge, UK, 2011).
[51] D. Janakiraman and K. L. Sebastian, Phys. Rev. E **86**, 061105 (2012).
[52] K. Goswami, Phys. Rev. E **99**, 012112 (2019).
[53] U. Seifert, Rep. Prog. Phys. **75**, 126001 (2012).
[54] K. Goswami, Physica A **525**, 223 (2019).
[55] G. E. Crooks, Phys. Rev. E **60**, 2721 (1999).
[56] D. Collin, F. Ritort, C. Jarzynski, S. B. Smith, I. Tinoco Jr, and C. Bustamante, Nature (London) **437**, 231 (2005).
[57] A. V. Chechkin and R. Klages, J. Stat. Mech. (2009) L03002.
[58] S. Chaki and R. Chakrabarti, Physica A **530**, 121574 (2019).
[59] R. A. Maller, G. Müller, and A. Szimayer, *Handbook of Financial Time Series* (Springer, Berlin, 2009), pp. 421–437.
[60] R. P. Feynman, A. R. Hibbs, and D. F. Styer, *Quantum Mechanics and Path Integrals* (Dover Publications, Oxford, UK, 2010).
[61] L. S. Schulman, *Techniques and Applications of Path Integration* (Courier Corporation, Boston, MA, 2012).